*International Geology Review*, Vol. 48, 2006, p. 1067–1086.


# Identification of UHP and Non-UHP Orthogneisses in the Sulu UHP Terrane, Eastern China: Evidence from SHRIMP U-Pb Dating of Mineral Inclusion–Bearing Zircons

FULAI LIU,[1]

*Institute of Geology, Chinese Academy of Geological Sciences, Beijing 100037, China*

J. G. LIOU,

*Department of Geological and Environmental Sciences, Stanford University, Stanford, California 94305*

AND HUAIMIN XUE

*Institute of Geology, Chinese Academy of Geological Sciences, Beijing 100037, China*



## Abstract

Mineral inclusions in zoned zircons reveal that both ultrahigh-pressure (UHP) and non-UHP orthogneisses occur in cores from drill hole CCSD-PP1 at Donghai, southwestern Sulu terrane. Zircons from the UHP orthogneiss have inherited magmatic cores containing low-P mineral inclusions, narrow mantles with UHP mineral inclusions, and rims that contain low-P minerals or are inclusion free. In contrast, zircons from non-UHP orthogneiss have only magmatic cores and metamorphic rims, both of which are characterized by low-P mineral inclusions, or are inclusion free. SHRIMP U-Pb analyses of zircons from the UHP orthogneiss identify three discrete and meaningful age groups: Proterozoic magmatic protolith ages >753 Ma in the cores, a UHP metamorphic event at 227 ± 8 Ma in the coesite-bearing mantles, and an amphibolite-facies overprint at 213 ± 7 Ma in the overgrowth rims. Zircons from non-UHP orthogneiss record only two discrete age groups, inherited magmatic cores with Proterozoic protolith ages >748 Ma, and metamorphic rims with an age of about 211 ± 6 Ma. The metamorphic rims have the same Triassic age as the late amphibolite-facies overprint of the UHP orthogneiss within analytical uncertainty.

These data, together with previous studies, suggest that Neoproterozoic supracrustal protoliths of the Yangtze craton experienced Late Triassic (227 ± 8 Ma) subduction to depths of at least 120 km, and were then rapidly exhumed to mid-crustal depths where both UHP rocks and a few non-UHP Neoproterozic granitic intrusives were subjected to coeval amphibolite-facies retrograde metamorphism at 211 ± 6 Ma. The exhumation rate deduced from the zircon age data and previously obtained metamorphic P-T data is estimated to be 6.3–7.1 km/m.y. This rapid exhumation suggests that the Sulu UHP metamorphic rocks returned to crustal depths as part of a buoyant sliver, possibly produced by slab breakoff.

## Introduction

SINCE DISCOVERY of the index UHP mineral coesite in meta-supracrustal rocks in the Western Alps (Chopin, 1984) and the Western Gneiss Region of Norway (Smith, 1984), UHP metamorphism has become the focus of worldwide study. Studies of UHP metamorphic rocks of supracrustal origin provide essential information on subduction and exhumation of continental crust, as well as on the dynamics of plate-tectonic processes at convergent margins. In the Dabie-Sulu UHP terrane of eastern China, inclusions of coesite, coesite pseudomorphs, trace diamonds, and other UHP metamorphic minerals are widespread but rare in eclogites (Okay et al., 1989; Wang and Liou, 1989; Hirajima et al., 1990; Xu S. et al., 1992, 2003, 2005; Liou and Zhang, 1996; Ye et al., 2000a), jadeite-bearing quartzites (Cong et al., 1995; Zhang et al., 1995a; Liou et al., 1997), metapelites + marbles (Wang and Liou, 1991; Schertl and Okay, 1994; Ye and Hirajima, 1996; Kato et al., 1997), and ultramafic rocks (Yang J. J. et al., 1993, 2000; Zhang et al., 1994, 2003a; Yang J. J., 2003).

[1]Corresponding author; email: liufulai@ccsd.cn

0020-6814/06/905/1067-20 $25.00

However, evidence of UHP metamorphism in Dabie-Sulu orthogneisses apparently has been obliterated by extensive retrograde metamorphism, and replaced by relatively low-P mineral assemblages during exhumation (Liu F. L. et al., 2004a). Therefore, whether these gneissic rocks were also subjected to UHP metamorphism is still disputed. Some geologists argue for tectonic emplacement of UHP eclogite bodies into low-P orthogneiss (Smith, 1988; Zhao Z. Y. et al., 1992; Okay and Sengör, 1992; Cong et al., 1995; Cong and Wang, 1999), whereas other workers consider that the eclogite and its host rocks experienced *in situ* UHP metamorphism (Wang and Liou, 1991; Wang et al., 1995; Zhang et al., 1995a; Ames et al., 1996; Liou et al., 1997, 2000; Liu F. L. et al., 2001, 2002, 2004a, 2004b; Zhang et al., 2003b). Recently, a few researchers have suggested that the Dabie-Sulu orthogneiss is a partial melting product of eclogitic rocks at the peak UHP metamorphic stage (You et al., 2004, 2005; Wallis et al., 2005).

Unfortunately, insufficient evidence is available in order to decide among these hypotheses. Coesite inclusions have been recently reported in zircon separates from some Dabie-Sulu orthogneisses, indicating the host rocks experienced UHP metamorphism (Tabata et al., 1998; Ye et al., 2000b; Liu J. B. et al., 2001). However, coesite has been found in only a few samples, and it is unclear whether all or most of the widely distributed orthogneisses experienced Triassic UHP metamorphism. A few non-UHP metamorphic units have also been identified in the Dabie-Sulu UHP terrane (Wu et al., 2004; Zhang et al., 2006; Liou et al., in press), but systematic studies of mineral inclusions in zircons and zircon ages have not been carried out to verify the extent of UHP metamorphism in this belt.

All Dabie-Sulu supracrustal rocks, including eclogite and its host rocks, have experienced a long, complex metamorphic history (Wang and Liou, 1991; Liou et al., 1997, 2000; Xu Z. Q. et al., 2003; Zhang et al., 2003b). Zircon, because of its chemical resistance and stability over a wide P-T range (Chopin and Sobolev, 1995; Liou et al., 1998; Parkinson and Katayama, 1999; Katayama et al., 2000, 2001; Parkinson, 2000; Liu F. L. et al., 2002), is the host mineral that most completely preserves coesite, diamond, silicic clinopyroxene, and other UHP phases. Zircon also plays an important role in geochronology. Sensitive High-Resolution Ion Micro-Probe (SHRIMP) dating of discrete domains within zircon crystals, combined with cathodoluminescence (CL) imaging, has contributed greatly to progress in dating Dabie-Sulu eclogite and gneissic rocks (Hacker et al., 1998; Maruyama et al., 1998; Cheng et al., 2000; Jian et al., 2000, 2001; Rumble et al., 2002; Zheng et al., 2003; Liu F. L. et al., 2004a).

The Dabie-Sulu zircon grains have had a complicated growth history as indicated by well-defined cores, mantles, and rims of zoned grains (Liu F. L. et al., 2002, 2004a). However, explaining the geological significance of SHRIMP U-Pb ages from different zircon domains is still difficult. Cheng et al. (2000) identified weighted mean ages of 757 ± 7 ($1\sigma$) and 223 ± 3 Ma ($1\sigma$) for zircon cores and rims, respectively, from Dabie eclogites, and interpreted the former as the UHP metamorphic age and the latter as an age modified by late-stage fluids. Jian et al. (2000, 2001) suggested that the UHP peak metamorphic age of the Xiongdian eclogite in the Dabie Mountains ranges from 480 to 424 Ma, whereas Hacker et al. (1998) reported UHP metamorphic ages of 224 ± 4 ($1\sigma$) and 236 ± 3 Ma ($1\sigma$) (weighted mean ages) of zircon rims from Dabie paragneiss and orthogneiss, respectively. Rumble et al. (2002) reported a 221 Ma zircon rim age for an orthogneiss, and 234–216 Ma ages for a garnet peridotite from southwestern Sulu. None of these studies differentiated the inherited UHP and retrograde overgrowth domains of zoned zircons through a study of mineral inclusions. Therefore, many of these reported SHRIMP dates may refer to different events.

In this paper, we identify mineral inclusions in zircons from core samples of orthogneiss in drill hole CCSD-PP1. The purposes of the study are to: (1) identify index UHP and low-P mineral inclusions; (2) determine the distribution of these inclusions in the zircon domains; (3) constrain the zircon growth history through CL imaging of the zircons; (4) distinguish non-UHP orthogneiss from UHP orthogneiss; and (5) conduct SHRIMP analyses to date various zircon domains of UHP and non-UHP orthogneiss. These data are then used to explain the geological significance of the discrete age groups and more precisely constrain the ages of UHP and amphibolite-facies retrograde metamorphism in the Dabie-Sulu UHP terrane.

## Geological Setting

The Sulu (Jiangsu-Shandong) orogen constitutes the eastern part of the Qinling-Dabie-Sulu orogen formed by the Triassic collision between the

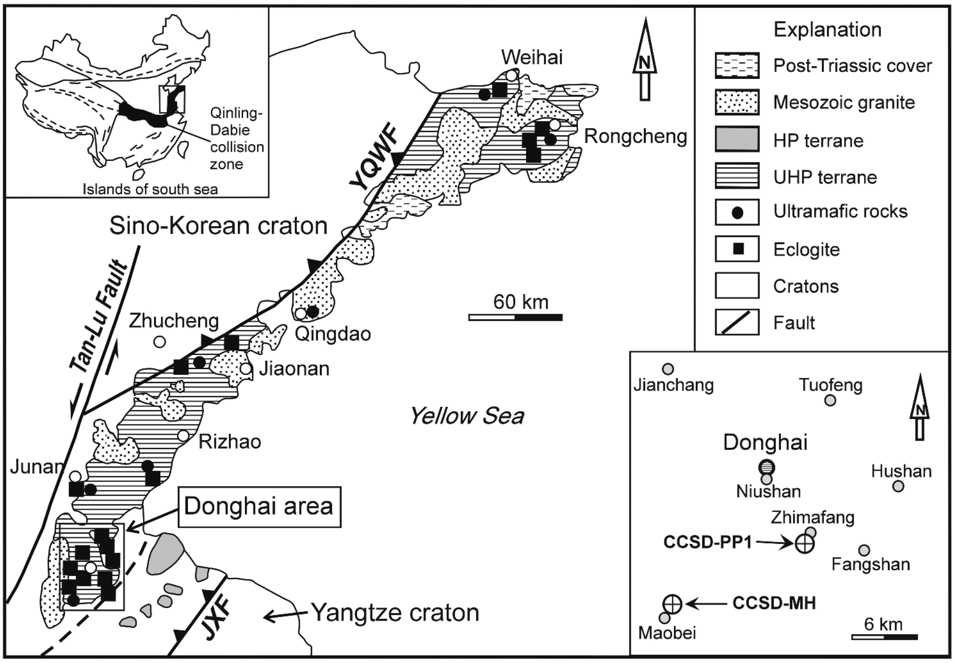


FIG. 1. Tectonic sketch map of the Sulu terrane and the Donghai area, showing major lithotectonic units and the locations of drill holes CCSD-PP1 and CCSD-MH. Abbreviations: YQWF = Yantai-Qingdao-Wulian fault.; JXF = Jiashan-Xiangshui fault.



Sino-Korean and Yangtze cratons (e.g., Ames et al., 1996; Hacker et al., 1998, 2004). The Sulu UHP and high-P belt, extending for about 320 km from Weihai, northeastern Shandong Province to Donghai of northern Jiangsu Province, is bounded by the Yantai-Qingdao-Wulian fault (YQWF) on the northwest and the Jiashan-Xiangshui fault (JXF) on the south (Fig. 1). The UHP belt consists mainly of amphibolite-facies orthogneiss, paragneiss, amphibolite, and marble, but some of the gneissic rocks and marbles contain abundant layers and blocks of eclogite. Many blocks of serpentinite, peridotite, and pyroxenite, ranging from a few meters to kilometers in size, are also present. Some garnetiferous peridotites and pyroxenites (Yang and Jahn, 2000; Yang J. J., 2003; Zhang et al., 2005; Zhao R. X. et al., 2005), and metagranitoids (Hirajiama et al., 1993) contain a record of Triassic UHP metamorphism. The high-P belt, southeast of the UHP belt contains mainly kyanite- and topaz-bearing quartzite, kyanite- and phengite-bearing quartzite, phengite-bearing quartz schist, phengite-bearing marble, epidote biotite albite gneiss, and rare blueschist (Zhang et al., 1995a, 2002; Liu F. L. et al., 2004a; Xu Z. Q. et al., 2004).

## Sample Locations and Petrography

Drill hole CCSD-PP1 is located near the village of Zhimafang, about 9 km southeast of Donghai County (Fig. 1). The hole was drilled to a depth of 432.0 m with more than 80% core recovery. The lithologic profile and selected zircon sample locations are shown in Figure 2. Six major lithologies were identified in the core: (1) eclogite, (2) ultramafic rock, (3) orthogneiss (granitic gneiss), (4) paragneiss, (5) kyanite quartz schist and epidote biotite schist, and (6) quartz veins. The detailed petrological characteristics of these rocks and of the mineral inclusions in zircons are described by Liu F. L. et al. (2001).

A garnet-biotite granitic gneiss (S3; 357 m depth) and an epidote-biotite granitic gneiss (S4; 23 m depth) were collected for the present study (Figs. 1 and 2). Sample S3 is light pink, coarse-grained, and consists mainly of K-feldspar + quartz + minor plagioclase, with subordinate (< 5%) garnet, biotite,

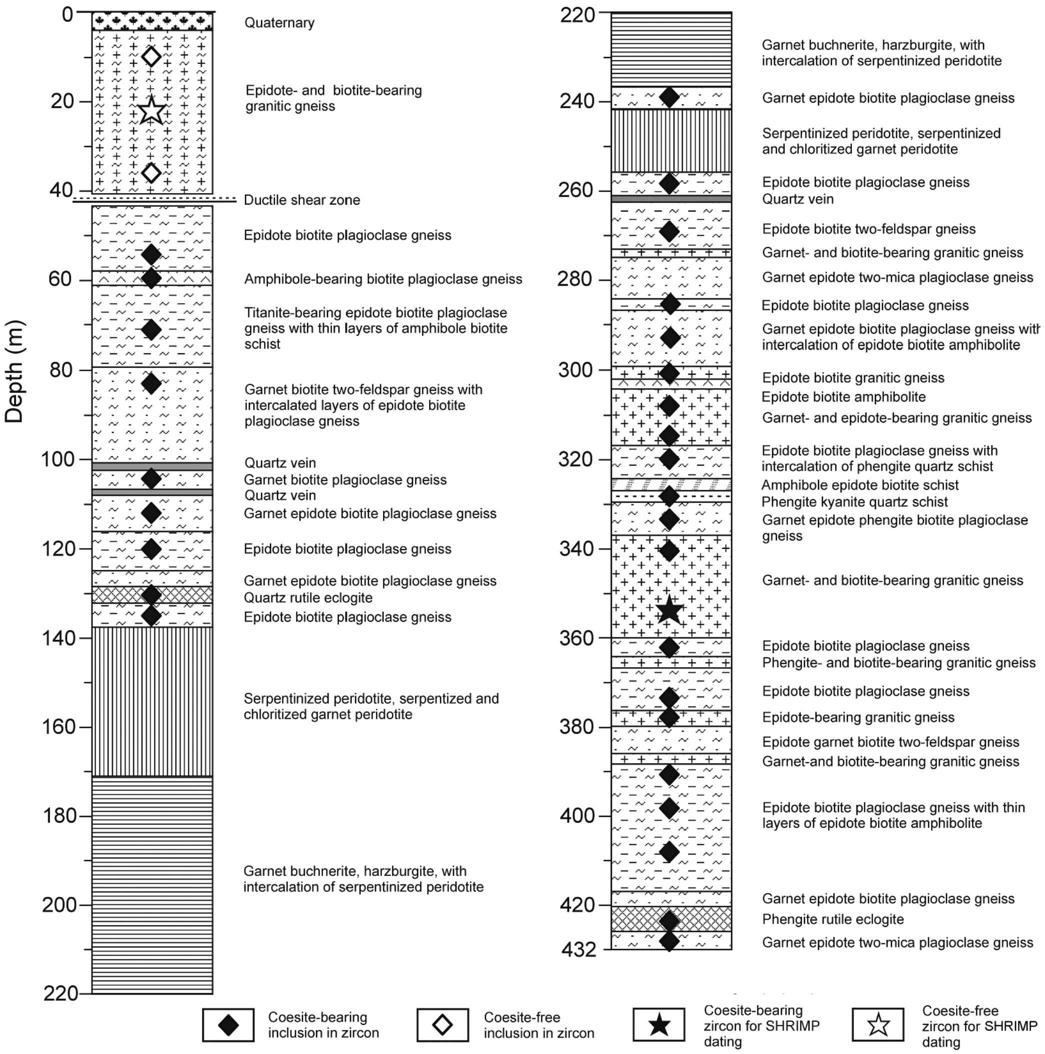


FIG. 2. The lithologic profile of the drill hole CCSD-PP1 in Zhimafang, southeastern Donghai. Locations of UHP mineral–bearing and non-UHP mineral–bearing zircons separated from core samples and locations of UHP and non-UHP zircons for the present SHRIMP U-Pb dating study are shown in the profile.

apatite, zircon, and ilmenite. The garnet is partially replaced by biotite. The S4 granitic gneiss is pale-colored, medium- to coarse-grained, and foliated. It consists of K-feldspar + plagioclase + quartz with subordinate (5%–10%) epidote, biotite, chlorite, apatite, zircon, and ilmenite. The alignment of biotite defines a weak foliation. Both samples record an amphibolite-facies metamorphic overprint.

A ductile shear zone at 41.0 m depth separates the CCSD-PP1 profile into two slices (Fig. 2). Both the upper slice (0–41.0 m) and the lower slice (41.0–432.0 m) experienced amphibolite-facies retrograde metamorphism related to exhumation of the Sulu terrane. A uniform deformational pattern has also been identified in both slices, with a NE-SW–trending foliation that dips 20–35° SE, and a SE-plunging stretching lineation (Xu Z. Q. et al., 2006).

## Analytical Techniques

Approximately 2 kg of each sample were crushed and sieved and the zircon separated with standard magnetic and heavy liquid techniques. Approximately 400 zircon grains from each sample were mounted and polished in 25 mm epoxy discs. Mineral inclusions in the zircons were analyzed using a RENISHAW-1000 Laser Raman spectroscope with the 514.5 nm line of an Ar-ion laser at the Institute of Geology, Chinese Academy of Geological Sciences (CAGS). The relationships between host zircon and inclusions were observed in detail using an optical microscope. Internal zoning patterns of the crystals were observed by cathodoluminescence (CL) image analysis at the microprobe laboratory of the Institute of Mineral Resources, CAGS. Mineral inclusion compositions were determined using a JEOL JXA 8800 electron microprobe with a 15 kV accelerating voltage and 20 nA beam current.

The zircons were analyzed for U, Th, and Pb using the SHRIMP II instrument at the Beijing Center, CAGS. Instrumental conditions and measurement procedures were the same as described by Compston et al. (1992). The spot size of the ion beam was about 25 μm in diameter, and the data were collected in sets of five scans through the masses with 2 nA primary $O_2^{-1}$ beams. The reference zircon was analyzed first and then again after every three unknowns. The measured $^{206}Pb/^{238}U$ ratios in the samples were corrected using reference zircon standard SL 13 from a pegmatite from Sri Lanka (572 Ma) and zircon standard TEMORA (417 Ma) from Australia (Black et al., 2003). The common-Pb correction used the $^{206}Pb/^{208}Pb$ ratio and assumed a two-stage evolution model (Stacey and Kramers, 1975). Analytical data are summarized in Tables 1 and 2, and graphically presented on Tera-Wasserburg (TW) diagrams with 1σ errors (see Figs. 5 and 6). The ages are weighted means with 1σ error calculated using isoplot at 95% confidence levels (Ludwig, 1991). Mineral abbreviations are after Kretz (1983).

## Microstructures and Micromineral Inclusions in Zircons

### *Garnet-biotite granitic gneiss (S3)*

Zircons separated from granitic gneiss (S3) contain mainly inclusions of coesite (Coe), garnet (Grt), phengite (Phe) or muscovite (Mus), quartz (Qtz), apatite (Ap), and K-feldspar (Kfs) (Table 1; Fig. 3). Most zircon crystals are light yellow to light brown, with dusty cores and colorless homogeneous mantles and rims. CL images of the analyzed zircons show low luminescent cores, bright luminescent mantles, and low luminescent rims (Figs. 3B, 3D, 3F, and 3H). However, delicate microtextures including irregular boundaries and various thicknesses of cores, mantles and rims of zoned zircons indicate the complexity of zircon growth. Most have a thick inherited core with an irregular mantle and rim (Figs. 3B, 3D, 3F and 3H). Some zircons have prismatic cores showing well-developed oscillatory zoning (Figs. 3B, 3D, 3F and 3H), and are considered to be magmatic in origin.

Most zircon grains have dusty cores that contain low-P mineral inclusions such as Qtz + Kfs + Ap (Fig. 3A), Qtz + Kfs + Mus + Ap (Figs. 3C and 3G), Qtz + Ap (Fig. 3E), and Qtz + Mus + Ap (Table 1). Coe (Figs. 3A, 3C and 3E), Coe + Phe (Fig. 3G), Coe + Grt (Table 1), Coe + Grt + Phe (Table 1), and Coe + Ap (Table 1) inclusions, which indicate UHP assemblages, are preserved only in zircon mantles. Some of the grains contain low-P minerals, such as Qtz (Fig. 3E; Table 1) in the rim, whereas others have inclusion-free rims (Figs. 3A, C and 3G; Table 1). The distinct zoning seen in the CL images and the distribution of mineral inclusions in zoned zircons suggest that: (a) euhedral zircon cores are igneous and represent the protolith; (b) mantles are UHP metamorphic overgrowths; and (c) rims formed by late-stage retrograde metamorphism.

### *Epidote-biotite granitic gneiss (S4)*

Zircon separates from granitic gneiss (S4) have euhedral prismatic habits with distinct oscillatory growth zoning formed during magmatic crystallization. Mineral inclusions in the zircons include quartz, K-feldspar, muscovite, calcite, and apatite (Fig. 4; Table 2). None of the 865 zircon grains examined from this and two other core samples from the depth interval of 4 to 41 m contain inclusions of index UHP minerals (e. g., coesite) (Fig. 4; Table 2). Based on their cathodoluminescence images (Figs. 4B, 4D, 4F, and 4H), the zircons are divided into two groups. The first group is characterized by nearly perfect euhedral crystal shapes (Figs. 4A and 4C) with well-developed zoning from core to rim (Figs. 4B and 4D), characteristic of crystallization from a magma. Mineral inclusions in these grains are mainly Qtz + Kfs + Cal + Ap (Fig. 4A), and Qtz + Kfs + Mus + Ap (Fig. 4C). None of these zircons have overgrowths around their magmatic cores, and they all maintain their primary crystal forms. In contrast, zircons of the second group have subhedral

TABLE 1. U-Th-Pb SHRIMP Zircon Data from UHP Orthogneiss (S3, 357 m depth) in Drill Hole CCSD-PP1, Chinese Continental Scientific Drilling Project[1]

| Sample | Zircon domain | Mineral inclusions | Content (ppm) U | Th | $Pb^{206}$ | Th/U | $^{206}Pb^*/^{238}U$ | $^{207}Pb^*/^{206}Pb^*$ | Age (Ma) $^{206}Pb^*/^{238}U$ | $^{207}Pb^*/^{206}Pb^*$ |
|---|---|---|---|---|---|---|---|---|---|---|
| S3-6.1 | Mantle | Coe, Grt | 112 | 5 | 4 | 0.04 | 0.0349 ± 0.0015 | 0.0500 ± 0.0034 | 221 ± 9 | 194 ± 152 |
| S3-6.2 | Rim | no | 68 | 13 | 2 | 0.20 | 0.0326 ± 0.0027 | 0.0575 ± 0.0032 | 207 ± 17 | 509 ± 115 |
| S3-14.1 | Core | Qtz, Ap | 76 | 42 | 7 | 0.54 | 0.0886 ± 0.0053 | 0.0543 ± 0.0050 | 548 ± 31 | 383 ±193 |
| S3-14.2 | Mantle | Coe | 191 | 20 | 7 | 0.11 | 0.0380 ± 0.0025 | 0.0572 ± 0.0056 | 240 ± 16 | 497 ± 202 |
| S3-14.3 | Rim | no | 50 | 10 | 1 | 0.20 | 0.0338 ± 0.0019 | 0.0488 ± 0.0033 | 214 ± 12 | 137 ± 78 |
| S3-20.1 | Mantle | Coe, Grt, Phe | 452 | 15 | 19 | 0.03 | 0.0348 ± 0.0017 | 0.0566 ± 0.0023 | 221 ± 11 | 476 ± 87 |
| S3-20.2 | Rim | Qtz | 638 | 19 | 19 | 0.03 | 0.0333 ± 0.0015 | 0.0510 ± 0.0016 | 211 ± 9 | 242 ± 69 |
| S3-25.1 | Core | Qtz, Kfs, Ap | 63 | 47 | 8 | 0.75 | 0.1172 ± 0.0044 | 0.0639 ± 0.0026 | 714 ± 25 | 737 ± 85 |
| S3-25.2 | Mantle | Coe | 76 | 12 | 3 | 0.15 | 0.0359 ± 0.0017 | 0.0510 ± 0.0033 | 227 ± 11 | 240 ± 112 |
| S3-25.3 | Mantle | Coe | 76 | 18 | 3 | 0.24 | 0.0360 ± 0.0017 | 0.0535 ± 0.0026 | 228 ± 10 | 351 ± 104 |
| S3-26.1 | Core | Qtz, Kfs, Mus, Ap | 315 | 268 | 43 | 0.85 | 0.1223 ± 0.0057 | 0.0679 ± 0.0041 | 744 ± 33 | 866 ± 119 |
| S3-26.2 | Mantle | Coe | 272 | 23 | 9 | 0.08 | 0.0357 ± 0.0017 | 0.0487 ± 0.0024 | 226 ± 11 | 135 ± 112 |
| S3-26.3 | Mantle | Coe | 387 | 13 | 13 | 0.03 | 0.0360 ± 0.0019 | 0.0567 ± 0.0042 | 228 ± 12 | 480 ± 155 |
| S3-30.1 | Mantle | Coe, Phe | 80 | 10 | 3 | 0.12 | 0.0350 ± 0.0016 | 0.0521 ± 0.0045 | 222 ± 10 | 291 ± 185 |
| S3-30.2 | Rim | no | 416 | 14 | 13 | 0.03 | 0.0333 ± 0.0032 | 0.0523 ± 0.0014 | 211 ± 20 | 300 ± 59 |
| S3-30.3 | Rim | no | 75 | 13 | 3 | 0.18 | 0.0339 ± 0.0016 | 0.0594 ± 0.0021 | 215 ± 10 | 580 ± 70 |
| S3-38.1 | Core | Qtz, Ap | 68 | 32 | 9 | 0.47 | 0.1236 ± 0.0048 | 0.0642 ± 0.0030 | 751 ± 27 | 747 ± 95 |
| S3-38.2 | Mantle | Coe | 73 | 13 | 2 | 0.18 | 0.0371 ± 0.0020 | 0.0586 ± 0.0030 | 235 ± 12 | 554 ± 105 |
| S3-38.3 | Mantle | Coe | 411 | 19 | 14 | 0.05 | 0.0360 ± 0.0021 | 0.0502 ± 0.0016 | 228 ± 13 | 203 ± 70 |
| S3-38.4 | Rim | Qtz | 117 | 29 | 4 | 0.25 | 0.0326 ± 0.0017 | 0.0566 ± 0.0028 | 207 ± 11 | 476 ± 104 |
| S3-41.1 | Mantle | Coe | 56 | 11 | 2 | 0.20 | 0.0351 ± 0.0020 | 0.0519 ± 0.0022 | 223 ± 12 | 283 ± 57 |
| S3-41.2 | Rim | no | 221 | 1 | 7 | 0.01 | 0.0341 ± 0.0014 | 0.0481 ± 0.0018 | 216 ± 8 | 106 ± 86 |
| S3-53.1 | Core | Qtz, Ap | 87 | 79 | 12 | 0.91 | 0.1092 ± 0.0014 | 0.0637 ± 0.0024 | 668 ± 36 | 732 ± 76 |
| S3-53.2 | Mantle | Coe, Grt | 356 | 9 | 11 | 0.03 | 0.0352 ± 0.0012 | 0.0534 ± 0.0019 | 223 ± 8 | 336 ± 81 |
| S3-53.3 | Rim | no | 318 | 9 | 10 | 0.03 | 0.0338 ± 0.0013 | 0.0505 ± 0.0026 | 214 ± 8 | 219 ± 115 |
| S3-66.1 | Core | Qtz, Kfs, Ap | 76 | 47 | 14 | 0.62 | 0.1119 ± 0.0033 | 0.0633 ± 0.0025 | 684 ± 38 | 720 ±84 |
| S3-66.2 | Mantle | Coe | 230 | 28 | 8 | 0.12 | 0.0352 ± 0.0014 | 0.0490 ± 0.0030 | 223 ± 8 | 150 ± 137 |
| S3-66.3 | Rim | no | 388 | 4 | 12 | 0.01 | 0.0341 ± 0.0011 | 0.0514 ± 0.0018 | 216 ± 7 | 258 ± 77 |
| S3-77.1 | Core | Qtz, Mus, Ap | 62 | 54 | 8 | 0.88 | 0.1239 ± 0.0107 | 0.0646 ± 0.0036 | 753 ± 61 | 762 ± 113 |
| S3-77.2 | Mantle | Coe, Phe | 334 | 9 | 11 | 0.03 | 0.0356 ± 0.0012 | 0.0519 ± 0.0022 | 226 ± 7 | 279 ± 96 |
| S3-77.3 | Mantle | Coe, Phe | 245 | 19 | 8 | 0.08 | 0.0358 ± 0.0013 | 0.0512 ± 0.0022 | 227 ± 8 | 248 ± 95 |
| S3-77.4 | Rim | no | 57 | 11 | 2 | 0.19 | 0.0331 ± 0.0014 | 0.0547 ± 0.0020 | 210 ± 9 | 401 ± 75 |
| S3-82.1 | Mantle | Coe | 298 | 14 | 9 | 0.05 | 0.0353 ± 0.0014 | 0.0481 ± 0.0018 | 224 ± 9 | 103 ± 87 |
| S3-82.2 | Rim | no | 98 | 14 | 3 | 0.15 | 0.0342 ± 0.0012 | 0.0497 ± 0.0041 | 217 ± 7 | 179 ± 173 |
| S3-98.1 | Core | Qtz, Mus, Ap | 115 | 93 | 22 | 0.81 | 0.0996 ± 0.0043 | 0.0612 ± 0.0031 | 612 ± 25 | 648 ± 87 |
| S3-98.2 | Mantle | Coe, Ap | 34 | 15 | 1 | 0.43 | 0.0375 ± 0.0034 | 0.0567 ± 0.0023 | 238 ± 21 | 481 ± 65 |
| S3-98.3 | Rim | no | 349 | 13 | 11 | 0.04 | 0.0346 ± 0.0013 | 0.0486 ± 0.0017 | 219 ± 8 | 130 ± 80 |

[1]Pb* corrected for common Pb using $^{208}Pb$. All errors are 1σ of standard deviation.

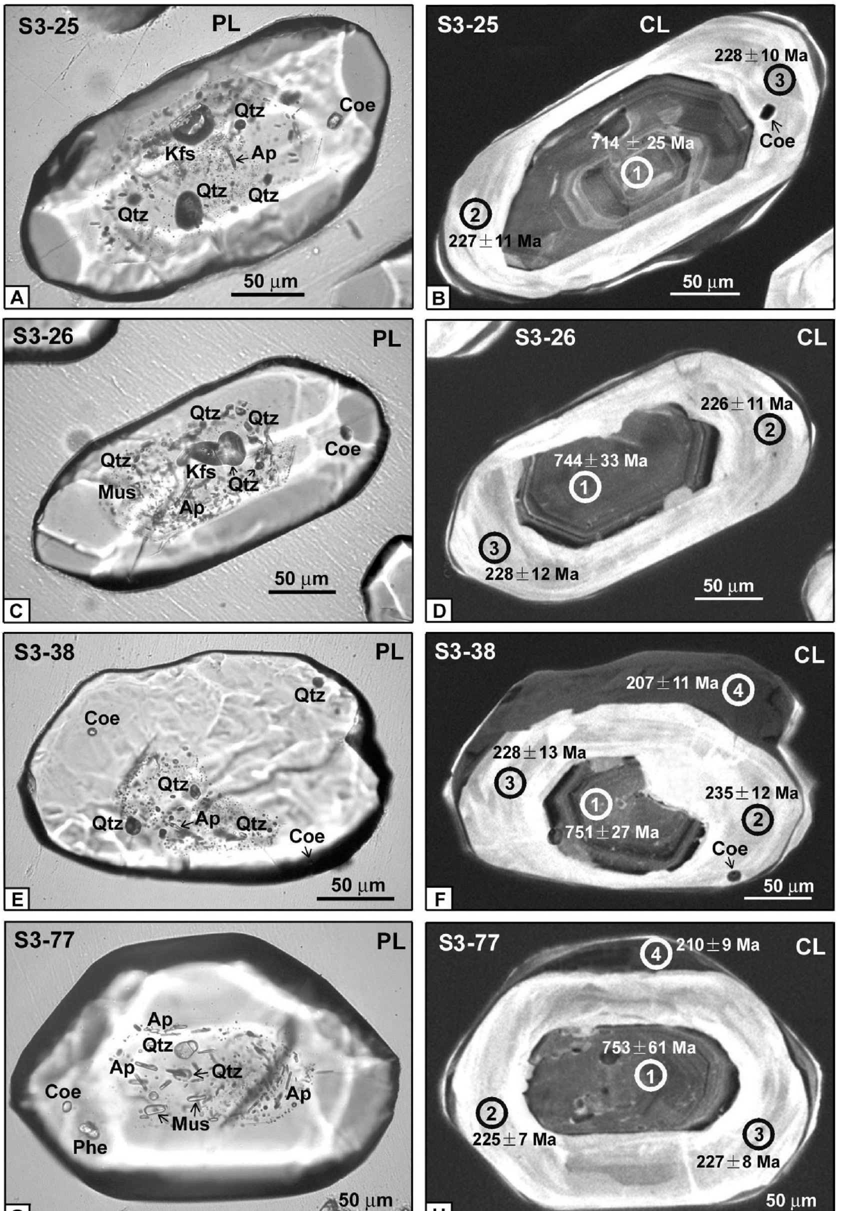


FIG. 3. Plane-polarized light (PL) images of mineral inclusions in zircon and CL images of host zircon from garnet-biotite granitic gneiss (UHP orthogneiss; S3, 357 m depth); the spots and ages of SHRIMP analysis of about 25 µm are also shown. A. Zircon grain S3-25 contains quartz + K-feldspar + apatite inclusion in the core, coesite in the mantle, and mineral inclusion-free in the rim. B. CL image of the same zircon as in A, showing core, mantle, and rim relationship and SHRIMP ages. C. Zircon grain S3-26 contains quartz + K-feldspar + muscovite + apatite inclusion in the core, coesite in the mantle, and mineral inclusion-free in the rim. D. CL image of the same zircon as in C, showing core, mantle, and rim relationship and SHRIMP ages. E. Zircon grain S3-38 contains quartz + apatite inclusion in the core, coesite in the mantle, and quartz in the rim. F. CL image of the same zircon as in E, showing core, mantle, and rim relationship and SHRIMP ages. G. Zircon grain S3-77 contains quartz + muscovite + apatite inclusion in the core, coesite + phengite in the mantle, and mineral inclusion-free in the rim. H. CL image of the same zircon as in G, showing core, mantle, and rim relationship and SHRIMP ages.

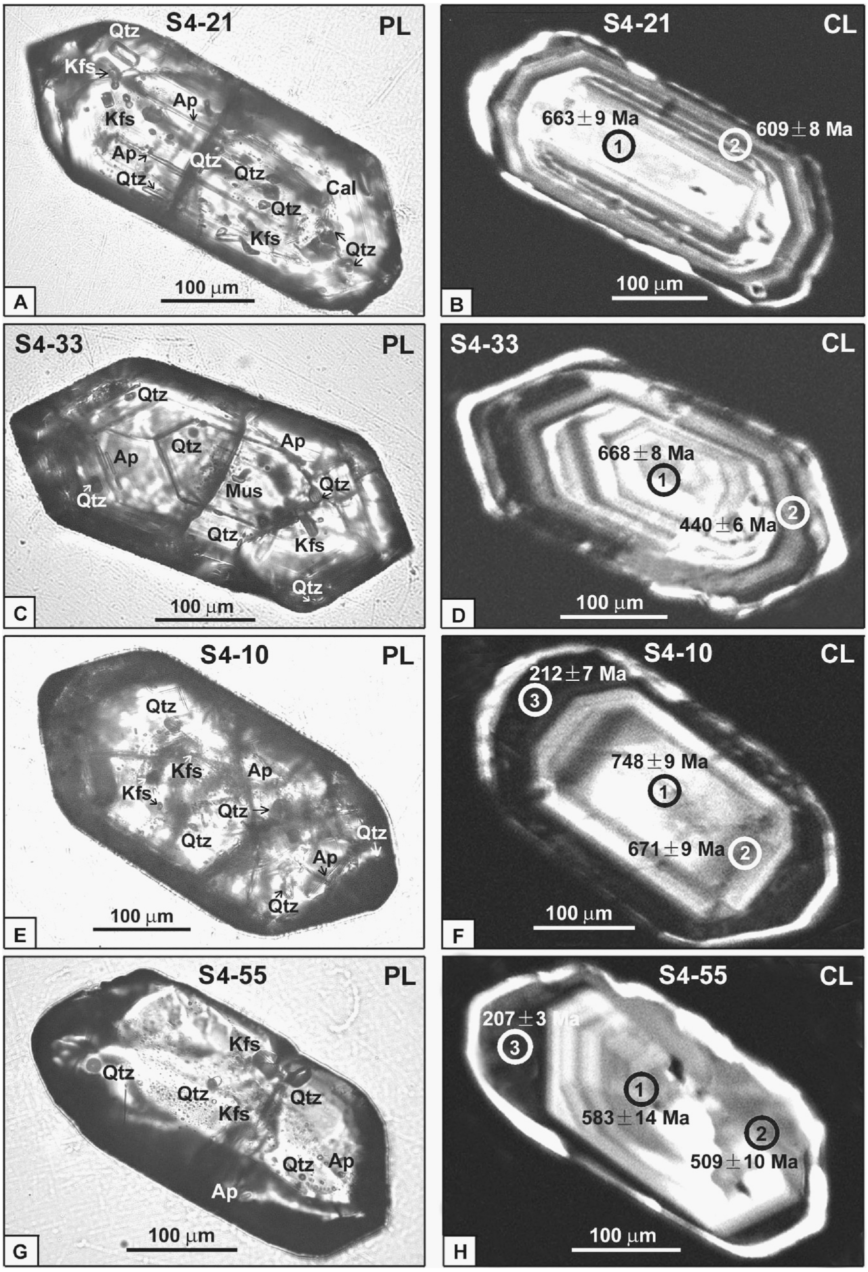


FIG. 4. Plane-polarized light (PL) images of mineral inclusions in zircon and CL images of host zircon from epidote-biotite granitic gneiss (non-UHP orthogneiss; S4, 23 m depth); the spots and ages of SHRIMP analysis of about 25 μm are also shown. A. Zircon grain S4-21 contains quartz + K-feldspar + calcite + apatite inclusion from the core to the rim. B. CL image of the same zircon as in A, showing magmatic zones and SHRIMP ages. C. Zircon grain S4-33 contains quartz + K-feldspar + muscovite + apatite inclusion from the core until the rim. D. CL image of the same zircon as in C, showing magmatic zones and SHRIMP ages. E. Zircon grain S4-10 contains quartz + K-feldspar + apatite inclusion in the core, and quartz in the rim. F. CL image of the same zircon as in E, showing inherited magmatic core and overgrowth rim relationship and SHRIMP ages. G. Zircon grain S4-55 contains quartz + K-feldspar + apatite inclusion in the core, and quartz in the rim. H. CL image of the same zircon as in G, showing inherited magmatic core and overgrowth rim relationship and SHRIMP ages.

TABLE 2. U-Th-Pb SHRIMP Zircon Data from non-UHP Orthogneiss (S4, 23 m depth) in Drill Hole CCSD-PP1, Chinese Continental Scientific Drilling Project[1]

| Sample | Zircon domain | Mineral inclusions | Content (ppm) U | Th | $Pb^{206}$ | Th/U | $^{206}Pb^*/^{238}U$ | $^{207}Pb^*/^{206}Pb^*$ | Age (Ma) $^{206}Pb^*/^{238}U$ | $^{207}Pb^*/^{206}Pb^*$ |
|---|---|---|---|---|---|---|---|---|---|---|
| S4-10.1 | Core | Qtz, Kfs, Ap | 328 | 276 | 16 | 0.87 | 0.1231 ± 0.0016 | 0.0651 ± 0.0008 | 748 ± 9 | 778 ± 29 |
| S4-10.2 | Core | | 431 | 197 | 14 | 0.47 | 0.1097 ± 0.0015 | 0.0660 ± 0.0011 | 671 ± 9 | 806 ± 34 |
| S4-10.3 | Rim | Qtz, Ap | 114 | 11 | 5 | 0.10 | 0.0334 ± 0.0012 | 0.0560 ± 0.0043 | 212 ± 7 | 450 ±174 |
| S4-12.1 | Core | Qtz, Kfs, Ap | 671 | 373 | 21 | 0.57 | 0.1053 ± 0.0017 | 0.0637 ± 0.0010 | 646 ± 10 | 733 ± 34 |
| S4-12.2 | Core | | 451 | 317 | 17 | 0.73 | 0.0796 ± 0.0012 | 0.0706 ± 0.0018 | 494 ± 7 | 945 ± 51 |
| S4-12.3 | Rim | Qtz | 87 | 5 | 7 | 0.06 | 0.0321 ± 0.0008 | 0.0550 ± 0.0048 | 204 ± 5 | 412 ± 175 |
| S4-16.1 | Core | Qtz, Ap | 806 | 429 | 23 | 0.55 | 0.0939 ± 0.0013 | 0.0665 ± 0.0023 | 578 ± 8 | 823 ± 71 |
| S4-16.2 | Core | | 743 | 474 | 16 | 0.66 | 0.0838 ± 0.0012 | 0.0640 ± 0.0015 | 519 ± 7 | 741 ± 52 |
| S4-16.3 | Rim | no | 235 | 16 | 7 | 0.07 | 0.0339 ± 0.0009 | 0.0522 ± 0.0019 | 215 ± 5 | 293 ± 95 |
| S4-21.1 | Core | Qtz, Kfs, Cal, Ap | 286 | 241 | 18 | 0.87 | 0.1084 ± 0.0015 | 0.0603 ± 0.0023 | 663 ± 9 | 615 ± 52 |
| S4-21.2 | Core | | 190 | 114 | 16 | 0.62 | 0.0991 ± 0.0014 | 0.0636 ± 0.0029 | 609 ± 8 | 728 ± 95 |
| S4-23.1 | Core | Qtz, Cal, Ap | 872 | 430 | 19 | 0.51 | 0.0933 ± 0.0011 | 0.0634 ± 0.0015 | 575 ± 7 | 723 ± 51 |
| S4-23.2 | Core | | 1589 | 340 | 26 | 0.22 | 0.0646 ± 0.0008 | 0.0611 ± 0.0023 | 404 ± 5 | 642 ± 79 |
| S4-23.3 | Rim | no | 376 | 13 | 4 | 0.04 | 0.0345 ± 0.0022 | 0.0535 ± 0.0010 | 219 ± 14 | 351 ± 43 |
| S4-24.1 | Core | Qtz, Cal, Ap | 247 | 183 | 19 | 0.77 | 0.1105 ± 0.0014 | 0.0661 ± 0.0012 | 676 ± 9 | 809 ± 38 |
| S4-24.2 | Core | | 190 | 114 | 14 | 0.62 | 0.1082 ± 0.0015 | 0.0632 ± 0.0018 | 663 ± 9 | 714 ± 59 |
| S4-24.3 | Rim | Qtz | 988 | 16 | 8 | 0.02 | 0.0329 ± 0.0009 | 0.0494 ± 0.0011 | 209 ± 3 | 166 ± 45 |
| S4-25.1 | Core | Qtz, Kfs, Ap | 287 | 207 | 12 | 0.75 | 0.0869 ± 0.0014 | 0.0559 ± 0.0045 | 537 ± 8 | 449 ± 180 |
| S4-25.2 | Rim | Qtz | 153 | 12 | 10 | 0.08 | 0.0333 ± 0.0008 | 0.0509 ± 0.0023 | 211 ± 5 | 234 ± 107 |
| S4-26.1 | Core | Qtz, Ap | 550 | 344 | 20 | 0.65 | 0.0947 ± 0.0012 | 0.0609 ± 0.0012 | 583 ± 7 | 636 ± 40 |
| S4-26.2 | Core | | 293 | 280 | 15 | 0.99 | 0.0844 ± 0.0026 | 0.0699 ± 0.0029 | 522 ± 16 | 927 ± 84 |
| S4-26.3 | Rim | Qtz | 261 | 15 | 10 | 0.06 | 0.0324 ± 0.0007 | 0.0518 ± 0.0018 | 206 ± 4 | 241 ± 26 |
| S4-26.4 | Rim | Qtz | 838 | 23 | 5 | 0.03 | 0.0284 ± 0.0005 | 0.0442 ± 0.0049 | 181 ± 3 | |
| S4-33.1 | Core | Qtz, Kfs, Ap, Mus | 636 | 365 | 17 | 0.59 | 0.1091 ± 0.0014 | 0.0630 ± 0.0013 | 668 ± 8 | 710 ± 44 |
| S4-33.2 | Core | | 503 | 256 | 22 | 0.53 | 0.0707 ± 0.0011 | 0.0641 ± 0.0019 | 440 ± 6 | 745 ± 64 |
| S4-35.1 | Core | Qtz, Ap | 523 | 313 | 13 | 0.62 | 0.0972 ± 0.0013 | 0.0663 ± 0.0015 | 598 ± 7 | 815 ± 45 |
| S4-35.2 | Core | | 499 | 686 | 16 | 1.42 | 0.0759 ± 0.0014 | 0.0626 ± 0.0038 | 472 ± 9 | 696 ± 130 |
| S4-35.3 | Rim | no | 266 | 12 | 4 | 0.05 | 0.0342 ± 0.0007 | 0.0533 ± 0.0022 | 217 ± 4 | 340 ± 93 |
| S4-40.1 | Core | Qtz, Kfs, Ap | 274 | 190 | 18 | 0.72 | 0.0981 ± 0.0016 | 0.0660 ± 0.0020 | 603 ± 9 | 806 ± 65 |
| S4-40.2 | Core | | 1766 | 3209 | 15 | 1.88 | 0.0816 ± 0.0011 | 0.0673 ± 0.0020 | 506 ± 7 | 847 ± 62 |
| S4-40.3 | Rim | Qtz, Ap | 520 | 3 | 7 | 0.01 | 0.0338 ± 0.0005 | 0.0605 ± 0.0054 | 214 ± 3 | 620 ± 212 |
| S4-55.1 | Core | Qtz, Kfs, Ap | 241 | 174 | 21 | 0.75 | 0.0946 ± 0.0024 | 0.0698 ± 0.0022 | 583 ± 14 | 924 ± 64 |
| S4-55.2 | Core | | 205 | 95 | 26 | 0.48 | 0.0821 ± 0.0016 | 0.0652 ± 0.0055 | 509 ± 10 | 781 ± 180 |
| S4-55.3 | Rim | Qtz, Ap | 690 | 4 | 14 | 0.01 | 0.0326 ± 0.0005 | 0.0466 ± 0.0021 | 207 ± 3 | 28 ± 97 |
| S4-60.1 | Rim | Qtz | 155 | 9 | 12 | 0.06 | 0.0326 ± 0.0012 | 0.0547 ± 0.0026 | 206 ± 8 | 402 ± 109 |

[1]Pb* corrected for common Pb using $^{208}Pb$. All errors are 1σ of standard deviation.

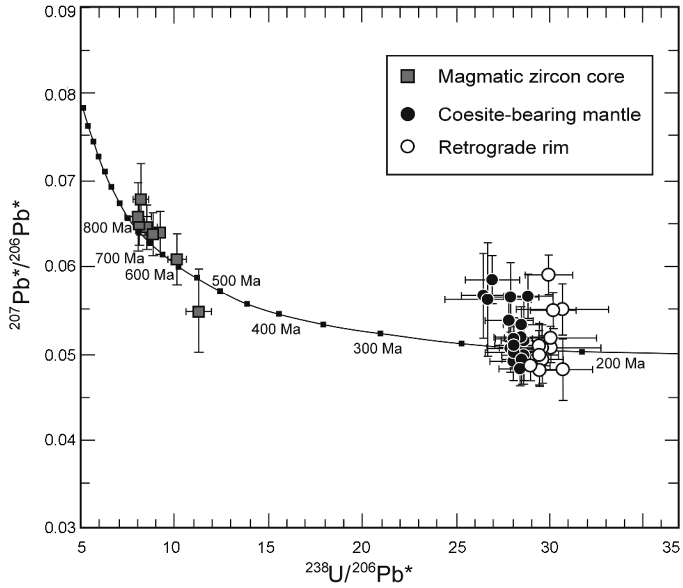


FIG. 5. TW diagram showing SHRIMP analyses of different zircon domains from garnet-biotite granitic gneiss (UHP orthogneiss; S3, 357 m depth).



crystal forms (Figs. 4E and 4G), with bright luminescent cores and low luminescent rims (Figs. 4F and 4H). Delicate microtextures, including irregular boundaries and variable thicknesses of cores and rims are also present. Most of these grains have a thick inherited core with an irregular rim (Figs. 4F and 4H). The cores are prismatic in form and show well-developed oscillatory zonings (Figs. 4F and 4H). They have a dusty appearance and contain only low-P mineral inclusion assemblages, such as Qtz + Kfs + Ap (Figs. 4E and 4G), Qtz + Cal + Ap (Table 2), and Qtz + Ap (Table 2). Some of the rims on these grains also contain low-P minerals, such as Qtz (Figs. 4E and 4G; Table 2), whereas others are inclusion-free (Table 1). Distinct zoning seen in the CL images and the distribution of mineral inclusions in these zircons suggest that: (a) the euhedral zircon cores are igneous and represent crystallization of the protolith; and (b) the rims formed by late-stage retrograde metamorphism related to exhumation of Sulu UHP terrane. No coesite or other UHP mineral inclusions were found in the zircons from orthogneiss samples from the 4-41 m interval of the drill core (Fig. 2), indicating that these orthogneisses were probably never subjected to UHP metamorphism.

## Results of SHRIMP U-Pb Zircon Dating

### *Results of SHRIMP U-Pb zircon dating of UHP orthogneiss*

Ion-microprobe data of 37 spots in 14 zircon grains from UHP orthogneiss, such as the garnet-biotite granitic gneiss (S3), are summarized in Table 1, and graphically plotted on Tera-Wasserburg diagrams with 1$\sigma$ errors (Fig. 5). All of the analyzed grains have a magmatic core, a coesite-bearing UHP mantle, and a retrograde rim (Fig. 3). Each of these domains has distinctive isotopic features (Table 1). The magmatic cores yield apparent $^{206}Pb^*/^{238}U$ ages ranging from 548 to 753 Ma (Table 1; Figs. 3 and 5), but show large variations in isotopic ratios (205 m.y. span between the oldest and youngest; Table 1). In general, the $^{207}Pb^*/^{206}Pb^*$ ages are older than the $^{206}Pb^*/^{238}U$ ages (Fig. 5; Table 1), indicating that these inherited zircon cores experienced Pb loss, and were also influenced by late thermal events. The zircon cores may have grown in the Proterozoic (>753 Ma; Fig. 5) and were influenced by later events. They are characterized by having higher Th values, and higher Th/U ratios, than the coesite-bearing mantles and retrograde rims (Table 1). The U and Th concentrations in the cores range

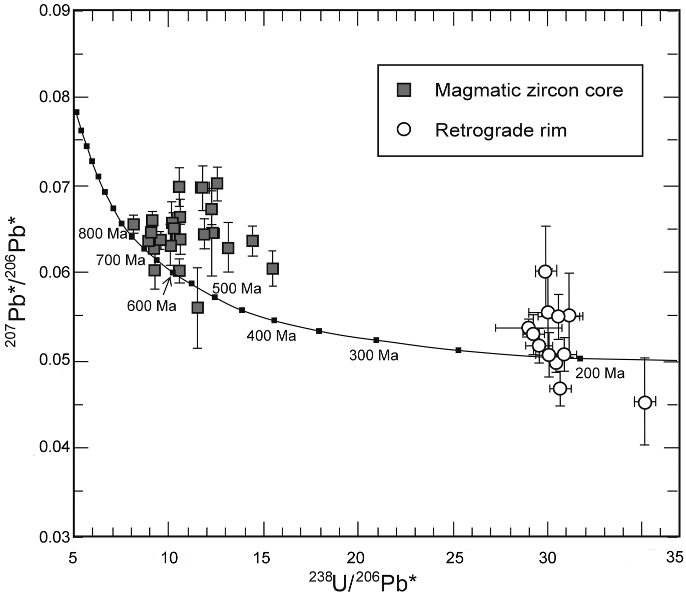


FIG. 6. TW diagram showing SHRIMP analyses of different zircon domains from epidote-biotite granitic gneiss (non-UHP orthogneiss; S4, 23 m depth).



from 62 to 315 ppm and 32 to 268 ppm, respectively, and the Th/U ratios range from 0.47 to 0.91 (Table 1). These features are similar to those of magmatic zircons from the Qinglongshan orthogneiss in the Donghai area (Rumble et al., 2002).

Seventeen spot analyses in the UHP mantles yield younger ages, ranging from 221 to 240 Ma (Table 1; Figs. 3 and 5). The weighted mean of the 17 measurements is 227 ± 8 Ma, with MSWD of 1.33. Compared to the zircon cores, the coesite-bearing mantles have distinctly lower Th values and Th/U ratios; the U and Th concentrations range from 34 to 452 ppm, and 5 to 28 ppm, respectively, giving Th/U ratios of 0.04–0.43 (Table 1). These compositions are similar to those of metamorphic zircon domains in UHP gneissic rocks from the southwestern Sulu UHP terrane (Rumble et al., 2002) and the Kokchetav massif (Hermann et al., 2001; Katayama et al., 2001). Thus, the ages of the analyzed coesite-bearing mantles are taken as the age of the UHP metamorphism in the Sulu terrane.

The zircon rims, which contain quartz inclusions, or are mineral inclusion–free, record the youngest ages; 12 analyzed spots have ages ranging from 207 to 219 Ma (Table 1; Figs. 3 and 5). The weighted mean of the 12 analyses is 213 ± 7 Ma, with MSWD of 0.66. The concentrations of U and Th, and the Th/U ratios, are similar to those of coesite-bearing metamorphic zircon domains; the U and Th values of rims range from 50 to 416 ppm, and 1 to 14 ppm, respectively, yielding distinctly low Th/U ratios of about 0.01–0.25 (Table 1). These low-P rims were formed during retrograde metamorphism related to exhumation of the Sulu terrane.

### *Results of SHRIMP U-Pb zircon dating of non-UHP orthogneiss*

Thirty-five spots were analyzed from 13 zircon grains from non-UHP epidote-biotite granitic gneiss (S4) in the same drill hole (Table 2, Figs. 4 and 6). Compared with the age data of UHP orthogneiss (Table 1; Fig. 5), SHRIMP U-Pb analyses of the zoned zircons from the non-UHP orthogneiss (S4) identify only two discrete and meaningful age groups (Table 2; Figs. 4 and 6). In the inherited cores of zircons with quartz, K-feldspar, calcite, and apatite inclusions, 23 analyses yield $^{206}Pb^*/^{238}U$ ages ranging from 440 to 748 Ma, indicating that these inherited zircon cores also experienced Pb loss and late metamorphic events. Therefore, the zircon cores probably grew in the Proterozoic, and the magmatic protolith age may be as old as 748 Ma (Fig. 6). Compared to the metamorphic overgrowth rims, the zircon cores are characterized by higher

Th values and higher Th/U ratios (Table 2). The U and Th concentrations and Th/U ratios range from 190 to 1589 ppm, 95 to 3209 ppm, and 0.22–1.88, respectively (Table 2). These features are similar to those of magmatic zircon cores separated from the UHP orthogneiss mentioned above (Table 1).

In the quartz-bearing and mineral inclusion–free overgrowth rims, 11 spot analyses yielded ages ranging from 204 to 219 Ma (only one spot was dated about 181 ± 3 Ma; Table 2; Figs. 4 and 6). The weighted mean $^{206}Pb^{*}/^{238}U$ age is 211 ± 6 Ma, with an MSWD of 2.3. These ages on the quartz-bearing and mineral inclusion-free rims are similar to those of zircon overgrowth rims in the UHP orthogneiss (Table 1; Fig. 5), and are considered to be the age of the late amphibolite-facies metamorphic event. Compared to the inherited zircon cores, the overgrowth rims are characterized by lower Th values and Th/U ratios (Table 2). The U and Th concentrations and Th/U ratios range from 87 to 838 ppm, 3 to 23 ppm, and 0.01–0.10, respectively (Table 2). These features are very similar to those of the retrograde rims on zircon grains in the UHP orthogneiss (Table 1).

## Discussion and Conclusions

Determination of the areal extent of UHP metamorphism is very important for tracing the subduction and exhumation of continental crustal rocks in the Dabie-Sulu orogen, studying the dynamics of tectonic processes at this convergent margin, and constructing geodynamic models of subduction and exhumation of the Dabie-Sulu terrane. However, the UHP metamorphic record of the gneissic rocks hosting the eclogite has been largely obliterated by subsequent retrograde recrystallization during rapid exhumation of the Dabie-Sulu terrane, making it very difficult to identify evidence of UHP metamorphism in these gneisses.

In recent years, geologists have focused on the study of mineral inclusions in zircons from both eclogite and gneiss in the Dabie-Sulu terrane, because zircon can preserve many primary UHP phases over a wide P-T range. Tabata et al. (1998) reported the presence of coesite inclusions in zircons from amphibolite-facies gneissic rocks at a number of widespread localities within the coesite-eclogite zone in the Dabie UHP terrane (Table 3), and Liu J. B. et al. (2001) identified coesite inclusions in zircons from gneissic rocks in the Wumiao-Shima area (Table 3). Of particular interest is the discovery of coesite inclusions in zircons from gneissic rocks of the "cold" eclogite zone that was previously considered to have not experienced UHP metamorphism. Wan et al. (2005) also found UHP minerals preserved in zircons from orthogneiss cobbles in the Heifei Basin, indicating that these cobbles were derived from the Dabie terrane. In the Sulu UHP terrane, recent studies have shown that inclusions of coesite and other UHP minerals are widespread in zircons of amphibolite-facies supracrustal rocks, including paragneiss, orthogneiss, amphibolite, marble, quartzite, and eclogite (Liu F. L. et al., 2004a; Table 3), and in zircons from core samples from drill holes CCSD-PP1 and CCSD-PP2 (Liu F. L. et al., 2001, 2002, 2003; Table 3). In addition, Ye et al. (2000b) and Yang J. S. et al. (2003) identified coesite inclusions in zircons from orthogneiss and peridotite in northeastern Sulu (Table 3). The widespread occurrence of coesite-bearing eclogites and gneisses in the Dabie-Sulu terrane suggests that passive-margin lithologies of the Yangtze craton were subducted to mantle depths, where they experienced coeval UHP metamorphism, and were then exhumed and overprinted by amphibolite-facies retrograde metamorphism.

More than 25 grains of diamond, ranging in size from 150 to 700 μm, have been recovered from Dabie-Sulu eclogites (Xu S. et al., 1992, 2003; Okay, 1993). The microdiamonds were positively identified by single-crystal X-ray diffraction and *in situ* laser Raman spectrometry. Recently, Xu S. et al. (2005) identified microdiamond inclusions in garnets from a few eclogite samples in the Dabie Mountains and the southwestern part of the Sulu terrane. They used infrared spectroscopy to determine that all the microdiamonds from the Dabie-Sulu terrane are mixed IaA and IaB types, thus ruling out the possibility of anthropogenic contamination.

On the other hand, we have investigated many core samples from drill holes CCSD-PP1, -PP2, and -MH (Liu F. L. et al., 2001, 2002, 2004b), and many outcrop samples of eclogite, amphibolite, paragneiss, orthogneiss, marble, quartzite, and schist from the southwestern Sulu terrane (Liu F. L. et al., 2003, 2004a) and failed to find any diamonds. Coesite inclusions, however, are present in zircons separated from more than 1000 core and surface samples. The absence of microdiamonds could reflect the relatively low $X_{CO_2}$ and high $f_{O_2}$ conditions deduced from mineral parageneses of these rocks (Zhang and Liou, 1997; Omori et al., 1998; Liou et al., 2002).

TABLE 3. Index UHP Minerals Identified as Inclusions in Zircons of Present and Previous Studies for Eclogite and Its Country Rocks in the Sulu-Dabie UHP Terrane

| UHP terrane | Locality | Rock type | UHP mineral inclusions | Reference |
|---|---|---|---|---|
| Sulu UHP terrane | Taohang, NE Sulu | Orthogneiss | Coe + Omp + Phe + Ttn | Ye et al., 2000 |
| | Drillhole CCSD-PP1, Zhimafang, SW Sulu | Paragneiss | Coe + Grt + Omp<br>Coe + Jd + Phe + Ap | Liu F. L. et al., 2001 |
| | | Amphibolite | Coe + Grt + Omp | Liu F. L. et al., 2003 |
| | | Orthogneiss | Coe + Phe + Rt<br>Coe + Grt + Phe + Ap | Liu F. L. et al., 2003 and this study |
| | Drillhole CCSD-PP2, Maobei, SW Sulu | Paragneiss | Coe + Grt + Omp + Rt<br>Coe + Grt + Jd + Phe + Ap | Liu F. L. et al., 2002 |
| | | Orthogneiss | Coe + Phe + Ap | |
| | | Amphibolite | Coe + Grt + Omp + Rt<br>Coe + Mgs | Liu F. L. et al., 2003 |
| | Weihai, NE Sulu | Peridotite | Coe + Grt + Phe + Rt | Yang J. S. et al., 2003 |
| | Donghai-Linsu, SW Sulu | Paragneiss | Coe + Grt + Omp + Phe<br>Coe + Jd + Grt + Phe + Rt + Ap | Liu F. L. et al., 2004a |
| | | Orthogneiss | Coe | |
| | | Quartzite | Coe + Grt + Omp + Ky + Phe + Ap | |
| | | Marble | Coe + Arg + Di | |
| | | Amphibolite | Coe + Grt + Omp + Phe + Rt + Ap | |
| | | Eclogite | Coe + Grt + Omp + Phe + Rt | |
| Dabie UHP terrane | Changpu-Shima-Wumiao | Paragneiss | Coe + Jd + Rt<br>Coe + Jd + Phe + Rt | Tabata et al., 1998 |
| | Wumiao-Shima | Orthogneiss | Coe + Phe | Liu J. B. et al., 2001 |
| | | Paragneiss | Coe + Omp + Phe + Ap | |
| | Heifei Basin | Orthogneiss cobble | Coe + Grt + Omp + Phe + Ap | Wan et al., 2005 |



As described in this paper (Fig. 4; Table 2) and by previous investigators (Wu et al., 2004; Zhang et al., 2006), it seems likely that at least some Dabie-Sulu orthogneisses were not subjected to Triassic UHP metamorphism. In spite of extensive search, no UHP inclusions have been found in zircons from orthogneiss in Fangshan, southern Sulu (Fig. 1) (Liu F. L. et al., 2001). These orthogneiss bodies (or blocks) might represent granitic intrusives that only underwent regional amphibolite-facies metamorphism at crustal depths during exhumation of the Dabie-Sulu UHP slabs.

Coesite-bearing UHP mineral inclusions are common in zircons from garnet-biotite granitic gneiss (S3) in drill hole CCSD-PP1 (Fig. 3; Table 1). The distribution of mineral inclusions in these zoned zircons records three stages of formation; Neoproterozoic magmatic crystallization (Fig. 7, Stage 1), UHP metamorphism at 227 ± 8 Ma (Fig. 7, Stage 2), and retrograde metamorphism at 213 ± 7 Ma (Fig. 7, Stage 3). In contrast, the SHRIMP ages of zoned zircons from the non-UHP orthogneiss (S4) yield two discrete age groups: Neoproterozoic magmatic crystallization (Fig. 7, Stage 1), and 211 ± 6 Ma for retrograde metamorphism (Fig. 7, Stage 3). The magmatic zircon cores with ages > 748 Ma are similar in age to the inherited magmatic zircon cores in the UHP orthogneiss. In addition, Liu F. L. et al. (2004b) obtained SHRIMP U-Pb ages of 810–910 Ma for the protolith of an UHP orthogneiss (R498) from a depth of 1325.2 m in drill hole CCSD-MH. Similar well-constrained Late Proterozoic ages for

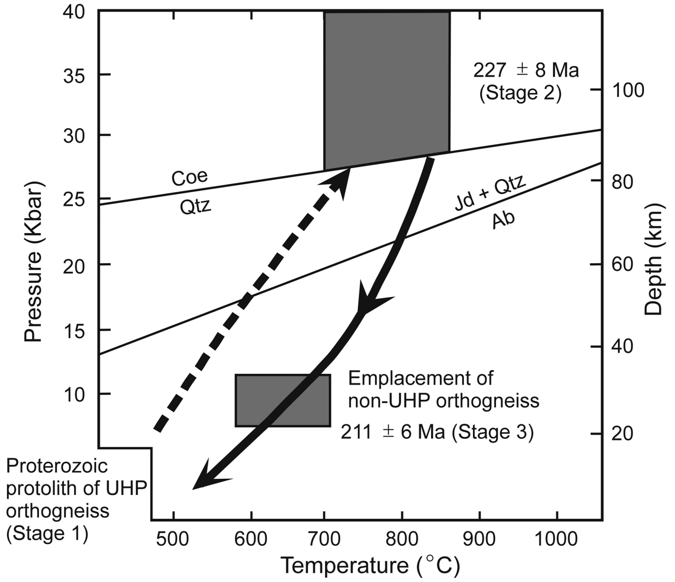


FIG. 7. Summarized P-T-time path for UHP metamorphic rocks of the southwestern Sulu terrane. The P-T path is derived from previous studies of Liu et al. (2001) and the present study. The SHRIMP analyses of different zircon domains yield three discrete stages of zircon growth: Proterozoic protolith age (Stage 1), 227 ± 8 Ma for the UHP metamorphic stage (Stage 2), and 211 ± 7 Ma for the retrograde stage (Stage 3) and the emplacement of non-UHP orthogneiss. The reaction curves of coesite (Coe) = quartz (Qtz) and jadeite (Jd) + quartz (Qtz) = albite (Ab) are from Bohlen and Boettcher (1982) and Holland (1980), respectively.

protoliths of UHP orthogneisses have also been reported by others—e.g., 731–831 Ma for Sulu by Ames et al. (1993, 1996) and Li et al. (1993), 638 to 722 Ma for Dabieshan by Ames et al. (1996) and Rowley et al. (1997), and up to 850 Ma for Dabieshan by Hacker et al. (1998).

Triassic UHP metamorphism in the Dabie-Sulu UHP terrane has been documented by numerous U-Pb, Sm-Nd, Rb-Sr, and Ar-Ar isotopic ages ranging from 245 to 210 Ma (e. g., Li et al., 2000; Zheng et al., 2003). However, controversy still exists over the exact timing of UHP metamorphism, and whether it occurred in the Early–Middle Triassic or Late Triassic. For example, the U-Pb isotopic data of Rowley et al. (1997) for zircons from granitoid gneiss in Dabie define a discordia with a lower intercept at 218.5 ± 1.7 Ma, interpreted by them as the age of UHP metamorphism. In contrast, Zheng et al. (2003) reported that UHP peak metamorphic ages of the Dabie-Sulu UHP terrane range from 240 to 245 Ma. Maruyama et al. (1998) obtained ages of 220–238 Ma by SHRIMP U-Pb dating of the cores of zircon grains from Dabie paragneiss, and interpreted these as the age of UHP metamorphism. Also, Rumble et al. (2002) reported a 221 Ma date for a zircon rim from an orthogneiss, and 216 to 236 Ma for zircon from a garnet peridotite from southwestern Sulu. However, on the basis of SHRIMP zircon data, Hacker et al. (1998) argued that the range of U-Pb dates from 209 to 243 Ma might imply zircon recrystallization in Dabie gneisses not only during the UHP metamorphism but also during retrograde metamorphism.

If zircons continue to grow during retrograde metamorphism, the lower intercept ages obtained by U-Pb zircon isotope dilution and zircon rim SHRIMP U-Pb ages would not accurately represent the UHP age. In our studies, coesite-bearing overgrowths on zircons from UHP garnet- and biotite-bearing granitic gneiss (S3) yield a SHRIMP U-Pb age of 227 ± 8 Ma. This UHP metamorphic age is similar to that of coesite-bearing zircon domains from an orthogneiss core (227 ± 2 Ma) in drill hole CCSD-MH (Liu F. L. et al., 2004b). Therefore, the weighted mean 227 ± 8 Ma for the coesite-bearing mantles of zircons in the UHP orthogneiss (S3) is clearly related to the UHP metamorphic event. This UHP age is also in agreement with several reported Sm-Nd ages of 221 to 228 Ma for adjacent coesite-bearing eclogite in the south-western Sulu terrane (Li et al., 1993, 1996).

Various P-T calculations of UHP eclogite and its host paragneiss and orthogneiss from drill hole CCSD-PP1 are shown in Figure 7 (Liu F. L. et al., 2001). Coesite in the eclogite and coesite inclusions in zircon from paragneiss and orthogneiss in the drill hole constrain the peak pressure to ≥ 28 kbar. The occurrence of diamond in the Maobei eclogite near drill hole CCSD-PP1 indicates that the minimum peak pressure could be as high as ~40 kbar (Xu S. et al., 2005). Using the garnet-clinopyroxene geothermometer, the peak temperatures have been estimated to range from 700 to 850°C for eclogite and paragneiss from drill hole CCSD-PP1 (Liu F. L. et al., 2001).

The 213 ± 7 Ma age corresponding to the amphibolite-facies overprint is recorded in the overgrowth rims of zircons from UHP garnet-biotite granitic gneiss (S3). These rims around the coesite-bearing mantles all contain low-P inclusions such as quartz (Table 1; Fig. 3). The replacement of garnet by biotite and amphibole + sodic plagioclase in orthogneiss and paragneiss (Liu F. L. et al., 2001) and symplectites of amphibole and plagioclase after omphacite and garnet in eclogite, indicates that these rocks experienced retrograde amphibolite-facies metamorphism (Liu F. L. et al., 2003). The reported U-Pb lower-intercept ages (Ames et al., 1993; Li et al., 2000) from 202 to 217 Ma in UHP rocks from southwestern Sulu may date this amphibolite-facies event. These ages are similar to those of the zircon rims of 207–219 Ma (Table 1) and 203–215 Ma for the UHP orthogneiss in CCSD-PP1 and CCSD-MH (Liu F. L. et al., 2004b), respectively. These data are also consistent with $^{40}Ar/^{39}Ar$ plateau ages (ranging from 200 to 219 Ma) of biotite separated from gneissic samples in drill hole CCSD-MH (Xu Z. Q. et al., 2006). In addition, the retrograde rims of zircons in the non-UHP orthogneiss (S4) in drill hole CCSD-PP1 have ages of 204–219 Ma (the weighted mean is 211 ± 6 Ma). These data indicate that both UHP and non-UHP orthogneisses simultaneously experienced an amphibolite-facies retrograde metamorphism; the emplacement age for the non-UHP orthogneiss intrusives into the Sulu-Dabie UHP metamorphic rocks is well constrained at 211 ± 6 Ma (Fig. 7, Stage 3).

Retrograde recrystallization is represented by the transition from coesite-bearing mineral inclusions in the mantles of zircons to quartz-bearing inclusions in the zircon rims (Table 1; Figs. 3E and 3F). Using the retrograde minerals only, it is difficult to estimate the temperature conditions of this stage due to the lack of appropriate geothermometers. However, garnet and omphacite have been partly or completely replaced by a symplectite of fine-grained hornblende and sodic plagioclase in the matrix of eclogite and amphibolite from drill hole CCSD-PP1 (Fig. 2); coexisting hornblende and sodic plagioclase in pseudomorphs after garnet and omphacite yield temperatures of 580–700°C using the Hbl-Pl thermometer (Blundy and Holland, 1990). Coexisting garnet, hornblende, and sodic plagioclase also yield similar temperatures of 650–710°C and pressures of 8–12 kbar using the Grt-Hbl-Pl-Qtz thermometer (Kohn and Spear, 1989). These estimates are consistent with the retrograde temperatures of 550–720°C and pressures of 8–12 kbar for the recrystallization of hornblende and plagioclase in eclogites (Enami and Zang, 1993; Zhang et al., 1995b). The results indicate that the temperature and pressure conditions for emplacement of non-UHP orthogneiss in Sulu UHP terrane were 580–710°C and 8–12 kbar, respectively (Fig. 7, Stage 3).

A speculative P-T-time path for zoned zircons from the UHP and non-UHP orthogneiss is shown in Figure 7, which provides a model for the tectonic evolution of the Sulu UHP terrane. Proterozoic continental protoliths, including granitic crustal materials, minor mafic-ultramafic rocks, and some passive-margin sediments (Fig. 7, Stage 1), were subducted to mantle depths in excess of 120 km and experienced UHP metamorphism during the Late Triassic (with a mean age of 227 ± 8 Ma). Some ultramafic-mafic intrusives of the mantle wedge may have been incorporated into the subduction zone because they possess mantle signatures (for review, see Zhang and Liou, 1998; Zhang et al., 2003a). Coesite-bearing UHP minerals crystallized and were trapped as inclusions in zircons at that time (Fig. 7, Stage 2). About 14–16 million years later, the deeply subducted UHP metamorphic rocks returned to mid-crustal levels. At these depths, some non-UHP orthogneiss intrusives of Yangtze affinity were tectonically emplaced into the UHP metamorphic terrane. Then, both UHP metamorphic rocks and non-UHP orthogneiss were subjected to an intense amphibolite-facies overprint (Fig. 7, Stage 3). Quartz and other low-P minerals formed at this time as inclusions in the zircon rims (Figs. 3 and 4).

Various mechanisms have been proposed to exhume UHP metamorphic rocks from mantle depths (Ernst, 1971; Zhang et al., 1995a; Hacker et al., 1996; Liou et al., 2000), and these have been widely applied to the Dabie-Sulu UHP terrane. Considering the weighted mean ages of UHP metamorphism and the subsequent amphibolite-facies retrograde event, about 14–16 m.y. elapsed from emplacement at diamond- and coesite-stable mantle depths to mid-crustal depths (Fig. 7). This suggests that about 100 km of exhumation must have occurred within 14 and 16 m.y., resulting in an average exhumation rate of 6.3–7.1 km/m.y., which is similar to that (~6.7 km/m.y.) for orthogneiss in drill hole CCSD-MH (Liu F. L. et al., 2004b). Rapid exhumation has been considered to be one of the most important factors in the preservation of UHP minerals (Wang and Liou, 1989; Liou and Zhang, 1996). The common occurrence of UHP minerals in Sulu metamorphic rocks suggests subduction to mantle depths in excess of 120 km and UHP metamorphism of voluminous continental materials (Liu F. L. et al., 2004a, 2004b). Because these continental materials have lower densities than the adjacent mantle peridotites, extrusion of the subducted wedge to mid-crustal levels during slab break-off may largely be due to buoyancy forces (Ernst and Liou, 1995; Liou et al., 2000). At mid-crustal depths, these UHP metamorphic rocks, together with some blocks of non-UHP orthogneiss, were overprinted by amphibolite-facies metamorphism.

## Acknowledgments

This manuscript results from our continuing study of mineral inclusions and SHRIMP geochronology of zircons from the Dabie-Sulu UHP rocks. We contribute this paper to the Liou Volume, which recognizes his contributions to the study of UHP metamorphism. We thank Prof. Liu Dunyi, Prof. Jian Ping, and Ms. Tao Hua for their generous help and discussion during the SHRIMP U-Pb dating of the zircons. This work has been funded by the Natural Science Foundation of China (grant No. 40399143), the National 973 Project of the Chinese Ministry of Science and Technology (grant No. 2003CB716502), and represents a joint effort of the Sino-American cooperative project supported by NSF EAR 0003355 and 0506901. The paper benefited from the constructive comments of Profs. P. Robinson, Qihan Shen, and Jingsui Yang. We thank the above-named individuals and institutes for their support and assistance.

## REFERENCES

Ames, L., Tilton, G. R., and Zhou, G., 1993, Timing of collision of the Sino-Korean and Yangtze cratons: U-Pb zircon dating of coesite-bearing eclogites: Geology, v. 21, p. 339–342.

Ames, L., Zhou, G., Xiong, B., 1996, Geochronology and isotopic character of high-pressure metamorphism with implications for collision of the Sino-Korean and Yangtze cratons, central China: Tectonics, v. 15, p. 472–489.

Black, L. P., Kamo, S. L., Allen, C. M., Aleinikoff, J. N., Davis, D. W., Korsch, R. J., and Foudoulis, C., 2003, TEMORA 1: A new zircon standard for Phanerozoic U-Pb geochronology: Chemical Geology, v. 200, p. 155–170.

Blundy, J. D., and Holland, T. J. B., 1990, Calcic amphibole-bearing equilibria and a new amphibole plagioclase geothermometer: Contributions to Mineralogy and Petrology, v. 104, p. 208–224.

Bohlen, S. R., and Boettcher, A. L., 1982, The quartz-coesite transformation: A pressure determination and effects of other components: Journal of Geophysical Research, v. 87, p. 7073–7078.

Cheng, Y. Q., Liu, D. Y., Williams, I. S., Jian, P., Zhuang, Y. X., and Gao, T. S., 2000, SHRIMP U-Pb dating of zircons of a dark-colored eclogite and garnet-bearing gneissic-granitic rock from Bixiling, eastern Dabie area, Anhui Province: Isotope chronogical evidence of Neoproterozoic UHP metamorphism: Acta Geologica Sinica, v. 74, p. 748–765.

Chopin, C., 1984, Coesite and pure pyrope in high-grade blueschist of the western Alps: A first record and some consequences: Contributions to Mineralogy and Petrology, v. 86, p. 107–118.

Chopin, C., and Sobolev, N., 1995, Principal mineralogic indicators of UHP in crustal rocks, *in* Coleman, R. G., and Wang, X., eds., Ultrahigh-pressure metamorphism: Cambridge, UK, Cambridge University Press, p. 96–131.

Compston, W., Williams, I. S., Kirschvink, J. L., Zhang, Z., and Ma, G., 1992, Zircon U-Pb ages for the early Cambrian time-scale: Journal of Geological Society, London, v. 149, p. 171–184.

Cong, B. L., and Wang, Q. C., 1999, A new review of Dabieshan-Sulu ultrahigh pressure belt: Chinese Science Bulletin, v. 44, p. 1127–1141.

Cong, B. L., Zhai, M. G., Carswell, D. A., Wilson, R. N., Wang, Q. C., Zhao, Z., and Windly, B. F., 1995, Petrogenesis of ultrahigh-pressure rocks and their country rocks at Shuanghe in Dabieshan, central China: European Journal of Mineralogy, v. 7, p. 119–138.

Enami, M., and Zang, Q. J., 1993, High-pressure eclogites in north Jiangsu–southern Shandong province, eastern China: Journal of Metamorphic Geology, v. 11, p. 589–603.

Ernst, W. G., 1971, Metamorphic zonations on presumably subducted lithospheric plates from Japan, California, and the Alps: Contributions to Mineralogy and Petrology, v. 34, p. 45–59.

Ernst, W. G., and Liou, J. G., 1995, Contrasting plate-tectonic styles of the Qinling-Dabie-Sulu and Franciscan metamorphic belts: Geology, v. 23, p. 353–356.

Hacker, B. R., Ratschbacher, L., and Liou, J. G., 2004, Subduction, collision, and exhumation in the Qinling-Dabie orogen: A review, *in* Malpas, J., ed., Aspects of the tectonic evolution of China: Geological Society of London, Special Paper 226, p. 157–175.

Hacker, B. R., Ratschbacher, L., Webb, L., Ireland, T., Walker, D., and Dong, S. W., 1998, U/Pb zircon ages constrain the architecture of the ultrahigh-pressure Qingling-Dabie orogen, China: Earth and Planetary Science Letters, v. 161, p. 215–230.

Hacker, B. R., Wang, X., Eide, E. A., and Ratschbacher, L., 1996, The Qinling-Dabie ultrahigh-pressure collisional orogen, *in* Yin, A., and Harrison, M. T., eds., The tectonic evolution of Asia: Cambridge, UK, Cambridge University Press, p. 345–370.

Hermann, J., Rubatto, D., and Korsakov, A., 2001, Multiple zircon growth during fast exhumation of diamondiferous, deeply subducted continental crust (Kokchetav Massif, Kazakhstan): Contributions to Mineralogy and Petrology, v. 141, p. 66–82.

Hirajima, T., Ishiwatari, A., Cong, B. L., Zhang, R. Y., Banno, S., and Nozaka, T., 1990, Coesite from Mengzhong eclogite at Donghai country, Northeastern Jiangsu Province, China: Mineralogical Magazine, v. 54, p. 579–583.

Hirajiama, T., Wallis, S. R., Zhai, M., and Ye, K., 1993, Eclogited metagranitoid from the Su-lu ultra-high pressure (UHP) province, eastern China: Progress in Japan Academy, v. 69B, p. 249–254.

Holland, T. J. B., 1980, The reaction albite = jadeite + quartz determined experimentally in the range 600–1200°C: American Mineralogist, v. 65, p. 129–134.

Jian, P., Liu, D. Y., Yang, W. R., and Williams, I. S., 2000, Petrographic and SHRIMP studies of zircons from the Caledonian Xiongdian eclogite, northwestern Dabie Mountains: Acta Geologica Sinica, v. 74, p. 766–773.

Jian, P., Liu, D. Y., Yang, W. R., and Williams, I. S., 2001, SHRIMP dating of zircons from the Caledonian Xiong-dian eclogite, western Dabie Mountains, China: Chinese Science Bulletin, v. 46, p. 77–79.

Katayama, I., Maruyama, S., Parkinson, C. D., Terada, K., and Sano, Y., 2001, Ion micro-probe U-Pb zircon geochronology of peak and retrograde stages of ultrahigh-pressure metamorphic rocks from the Kokchetav massif, northern Kazakhstan: Earth and Planetary Science Letters, v. 188, p. 185–198.

Katayama, I., Zayachkovsky, A. A., and Maruyama, S., 2000, Progressive P-T records from zircon in Kokchetav UHP-HP rocks, northern Kazakhstan: The Island Arc, v. 9, p. 417–427.

Kato, T., Enami, M., and Zhai, M., 1997, Ultra-high-pressure (UHP) marble and eclogite in the Su-lu UHP terrane, eastern China: Journal of Metamorphic Geology, v. 15, p. 169–182.

Kohn, M. J., and Spear, F. S., 1989, Empirical calibration of geobarometers for the assemblage garnet + hornblende + plagioclase + quartz: American Mineralogist, v. 74, p. 77–84.

Kretz, R., 1983, Symbols for rock-forming mineral: American Mineralogist, v. 68, p. 277–279.

Li, S. G., Jagoutz, E., Lo, C. H., Chen, Y., Li, Q., and Xiao, Y., 2000, Sm/Nd, Rb/Sr, and $^{40}Ar/^{39}Ar$ isotope systematics of ultrahigh-pressure metamorphic rocks in the Dabie-Sulu belt, central China: A retrospective view, *in* Ernst, W. G., and Liou, J. G., eds., Ultrahigh-pressure metamorphism and geodynamics in collision-type orogenic Belts: Columbia, MD: Bellwether Publishing, Ltd., p. 234–244.

Li, S. G., Jagoutz, E., Xiao, Y. L., Ge, N., and Chen, Y., 1996, Chronology of ultrahigh-pressure metamorphism in the Dabie mountains and Su-Lu terrane: Science in China (series D), v. 39, p. 597–609.

Li, S. G., Xiao, Y. L., Liu, D., Chen, Y., Ge, N., Zhang, Z., Sun, S. S., Cong, B. L., Zhang, R. Y., and Hart, S. R., 1993, Collision of the north China and Yangtze blocks and formation of coesite-bearing eclogites: Timing and process: Chemical Geology, v. 109, p. 89–111.

Liou, J. G., Hacker, B. R., and Zhang, R. Y., 2000, Into the forbidden zone: Science, v. 287, p. 1215–1216.

Liou, J. G., Tsujimori, T., Chu, W., Zhang, R. Y., and Wooden, J. L., in press, Late Archean to Paleoproterozoic history of the Haiyangsuo complex, eastern China: A non-UHP exotic tectonic slab in the Sulu ultrahigh-pressure terrane: Mineralogy and Petrology.

Liou, J. G., and Zhang, R. Y., 1996, Occurrence of intergranular coesite in Sulu ultrahigh-P rocks from China: implications for fluid activity during exhumation: American Mineralogist, v. 81, p. 1217–1221.

Liou, J. G., Zhang, R. Y., Ernst, W. G., Rumble, D., and Maruyama, S., 1998, High-pressure minerals from deeply subducted metamorphic rocks: Reviews in Mineralogy and Geochemistry, v. 37, p. 33–96.

Liou, J. G., Zhang, R. Y., and Jahn, B. M., 1997, Petrology, geochemistry and isotope data on a ultrahigh-pressure jadeite quartzite from Shuanghe, Dabie mountains, east-central China: Lithos, v. 41, p. 59–78.

Liou, J. G., Zhang, R. Y., Katayama, I., Maruyama, S., and Ernst, W. G., 2002, Peterotectonic characterization of the Kokchetav Massif and the Dabie-Sulu terranes: Ultrahigh-P metamorphism in the so-called forbidden zone: Western Pacific Earth Sciences, v. 2, p. 119–148.

Liu, F. L., Xu, Z. Q., Katayama, I., Yang, J. S., Maruyama, S., and Liou, J. G., 2001, Mineral inclusions in zircons of para- and orthogneiss from pre-pilot drillhole CCSD-PP1, Chinese Continental Scientific Drilling Project: Lithos, v. 59, p. 199–215.

Liu, F. L., Xu, Z. Q., and Liou, J. G., 2004a, Tracing the boundary between UHP and HP metamorphic belts in the southwestern Sulu terrane, eastern China: Evidence from mineral inclusions in zircons from metamorphic rocks: International Geology Review, v. 46, p. 409–425.

Liu, F. L., Xu, Z. Q., Liou, J. G., Katayama, I., Masago, H., Maruyama, S., and Yang, J. S., 2002, Ultrahigh-pressure mineral inclusions in zircons from gneissic core samples of the Chinese Continental Scientific Drilling Site in eastern China: European Journal of Mineralogy, v. 14, p. 499–512.

Liu, F. L., Xu, Z. Q., and Xue, H. M., 2004b, Tracing the protolith, UHP metamorphism, and exhumation ages of orthogneiss from the SW Sulu terrane (eastern China): SHRIMP U-Pb dating of mineral inclusion-bearing zircons: Lithos, v. 78, p. 411–429.

Liu, F. L., Zhang, Z. M., Katayama, I., Xu, Z. Q., and Maruyama, S., 2003, Ultrahigh-pressure metamorphic records hidden in zircons from amphibolites in Sulu terrane, eastern China: The Island Arc, v. 12, p. 256–267.

Liu, J. B., Ye, K., Maruyama, S., Cong, B. L., Fan, H. R., 2001, Mineral inclusions in zircon from gneisses in the ultrahigh-pressure zone of the Dabie Mountains, China: Journal of Geology, v. 109, p. 523–535.

Ludwig, K. R., 1991, Isoplot: A plotting and regression program for radiogenic isotope data: USGS Open-File Report, v. 1-455, 39 p.

Maruyama, S., Tabata, H., Nutman, A. P., Morikawa, T., Liou, J. G., 1998, SHRIMP U-Pb geochronology of ultrahigh-pressure metamorphic rocks of the Dabie Mountains, central China: Continental Dynamics, v. 3, p. 72–85.

Okay, A. I., 1993, Petrology of a diamond and coesite-bearing metamorphic terrane: Dabie Shan, China: European Journal of Mineralogy, v. 5, p. 659–675.

Okay, A. I., and Sengör, A. M. C., 1992, Evidence for intra-continental thrust related exhumation of the ultra-high pressure rocks in China: Geology, v. 20, p. 411–414.

Okay, A. I., Xu, S., and Sengör, A. M. C., 1989, Coesite from the Dabie Mountains eclogite, central China: European Journal of Mineralogy, v. 1, p. 595–598.

Omori, S., Liou, J. G., Zhang, R. Y., and Ogasawara, Y., 1998, Petrogenesis of impure dolomitic marble from the Dabie Mountains, central China: The Island Arc, v. 7, p. 98–114.

Parkinson, C. D., 2000, Coesite inclusions and prograde compositional zonation of garnets in whiteschists of the Kokchetav Massif, Kazakhstan: A unique record of progressive UHP metamorphism: Lithos, v. 52, p. 215–233.

Parkinson, C. D., and Katayama, I., 1999, Present day ultrahigh-pressure conditions of coesite inclusions in zircon and garnet: Evidence from laser Raman microspectroscopy: Geology, v. 27, p. 979–982.

Rowley, D. B., Xue, F., Tucker, R. D., Peng, Z. X., Baker, J., and Davis, A., 1997, Ages of ultrahigh-pressure metamorphism and protolith orthogneisses from the eastern Dabieshan: U-Pb zircon geochronology: Earth and Planetary Science Letters, v. 151, p. 191–203.

Rumble, D., Giorgis, D., Ireland, T., Zhang, Z. M., Xu, H. F., Yue, T. F., Yang, J. S., Xu, Z. Q., and Liou, J. G., 2002, $\delta^{18}O$ zircons, U-Pb dating, and the age of the Qinglongshan oxygen and hydrogen isotope anomaly near Donghai in Jiangsu Province, China: Geochimica et Cosmochimica Acta, v. 66, p. 2299–2306.

Schertl, H. P., and Okay, A. I., 1994, A coesite inclusion in dolomite in Dabie Shan, China: Petrological and rheological significance: European Journal of Mineralogy, v. 6, p. 995–1000.

Smith, D. C., 1984, Coesite in clinopyroxene in the Caledonides and its implications for geodynamics: Nature, v. 310, p. 641–644.

Smith, D. C., 1988, A review of the peculiar mineralogy of the "Norwegian coesite-eclogite province," with crystal-chemical, petrological, geochemical, and geodynamical notes and an extensive bibliography, *in* Smith, D. C., ed., Eclogites and eclogite-facies rocks: Amsterdam, The Netherlands, Elsevier, p. 1–126.

Stacey, J. S., and Kramers, J. D., 1975, Approximation of terrestrial lead isotope evolution by a two-stage model: Earth and Planetary Science Letters, v. 26, p. 207–221.

Tabata, H., Yamauchi, K., Maruyama, S., and Liou, J. G., 1998, Tracing the extent of a UHP metamorphic terrane: mineral inclusion study of zircons in gneisses from the Dabieshan, *in* Hacker, B. R., and Liou, J. G., eds., When continents collide: Geodynamics and geochemistry of ultrahigh-pressure rocks: Dordrecht, The Netherlands, Kluwer Academic Publishing, p. 261–273.

Wan, Y. S., Li, R. W., Wilde, S. M., Liu, D. Y., Chen, Z. Y., Yan, L., Song, T. R., and Yin, X. Y., 2005, UHP metamorphism and exhumation of the Dabie Orogen, China: Evidence from SHRIMP dating of zircon and monazite from a UHP granitic gneiss cobble from the Hefei basin: Geochimica et Cosmochimica Acta, v. 69, p. 4333–4348.

Wang, X., and Liou, J. G., 1989, Coesite-bearing eclogites from the Dabie mountains in central China: Geology, v. 1, p. 1085–1088.

Wang, X., and Liou, J. G., 1991, Regional ultrahigh-pressure coesite-bearing eclogitic terrane in central China: Evidence from country-rocks, gneiss, marble, and metapelite: Geology, v. 19, p. 933–936.

Wang, X., Zhang, R. Y., and Liou, J. G., 1995, Ultrahigh-pressure metamorphic terrane in eastern China, *in* Coleman, R. G., and Wang, X., eds., Ultrahigh-pressure metamorphism: Cambridge, UK, Cambridge University Press, p. 356–390.

Wallis, S., Tsuboi, M., Suzuki, K., Fanning, M., Jiang, L., and Tanaka, T., 2005, Role of partial melting in the evolution of the Sulu (eastern China) ultrahigh-pressure terrane: Geology, v. 33, p. 129–132.

Wu, Y. B., Zheng, Y. F., and Zhou, J. B., 2004, Neoproterozoic granitoid in northwest Sulu and its bearing on the north China-south China blocks boundary in east China: Geophysical Research Letters, v. 31, p. 1–4.

Xu, S., Liu, Y., Chen, G. B., Compagnoni, R., Rolfo, F., He, M. C., and Liu, H. F., 2003, New finding of micro-diamonds in eclogites from Dabie-Sulu region in central-eastern China: Chinese Science Bulletin, v. 48, p. 988–994.

Xu, S., Liu, Y., Chen, G. B., Ji, S. Y., Ni, P., and Xiao, W. S., 2005, Microdiamonds, their classification and tectonic implications for the host eclogites from the Dabie and Su-Lu regions in central eastern China: Mineralogical Magazine, v. 69, p. 509–520.

Xu, S., Okay, A. I., Ji, S., Sengor, A. M. C., Su, W., Liu, Y., and Jiang, L., 1992, Diamond from the Dabie Shan metamorphic rocks and its implication for tectonic setting, Science, v. 256, p. 8–12.

Xu, Z. Q., Zeng, L. S., Liu, F. L., Yang, J. S., Zhang, Z. M., McWilliams, M., and Liou, J. G., 2006, Polyphase subduction and exhumation of the Sulu HP-UHP metamorphic terrane, *in* Hacker, B. R., McClelland, B., and Liou, J. G., eds., Ultrahigh-pressure metamorphism: Deep continental subduction: Geological Society of America Special Paper, v. 403, p. 93–113.

Xu, Z. Q., Zhang, Z. M., Liu, F. L., Yang, J. S., Li, H. B., Yang, T. N., Qiu, H. J., Li, T. F., Meng, F. C., Chen, S. Z., Tang, Z. M., and Chen, F. Y., 2003, Exhumation structure and mechanism of the Sulu ultrahigh-pressure metamorphic belt, central China: Acta Geologica Sinica, v. 77, p. 433–450 (in Chinese with English abstract).

Xu, Z. Q., Zhang, Z. M., Liu, F. L., Yang, J. S., Tang, Z. M., Chen, S. Z., Chai, Y. C., Li, T. F., and Chen, F. Y., 2004, The structure profile of 0–2000 m in the main borehole, Chinese Continental Scientific Drilling and its preliminary deformation analysis: Acta Petrologica Sinica, v. 20, p. 53–72.

Yang, J. J., 2003, Titanian clinohumite-garnet-pyroxene rock from the Su-Lu UHP metamorphic terrane, China: Chemical evolution and tectonic implications: Lithos, v. 70, p. 359–379.

Yang, J. J., Godard, G., Kienast, J. R., Lu, Y., and Sun, J., 1993, Ultrahigh-pressure (60 kbar) magnesite-bearing garnet peridotites from north Jiangsu, China: Journal of Geology, v. 18, p. 541–554.

Yang, J. J., and Jahn, B. M., 2000. Deep subduction of mantle-derived garnet peridotites fron the Su-lu UHP metamorphic terrane in China: Journal of Metamorphic Geology, v. 18, p. 167–180.

Yang, J. S., Wooden, J. L., Wu, C. L., Liu, F. L., Xu, Z. Q., Shi, R. D., Katayama, I., Liou, J. G., and Maruyama, S., 2003, SHRIMP U-Pb dating of coesite-bearing zircon from the ultrahigh-pressure metamorphic rocks, Sulu terrane, east China: Journal of Metamorphic Geology, v. 21, p. 551–560.

Ye, K., Cong, B. L., and Ye, D. N., 2000a, The possible subduction of continental material to depths greater than 200 km: Nature, v. 407, p. 734–736.

Ye, K., and Hirajima, T., 1996, High-pressure marble at Yangguantun, Rongcheng County, Shandong Province, eastern China: Mineralogy and Petrology, v. 57, p. 151–165.

Ye, K., Yao, Y. P., Katayama, I., Cong, B. L., Wang, Q. C., and Maruyama, S., 2000b, Large areal extent of ultrahigh-pressure metamorphism in the Sulu ultrahigh-pressure terrane of east China: New implications from coesite and omphacite inclusions in zircon of granitic gneiss: Lithos, v. 52, p. 157–164.

You, Z. D., Su, S. G., Liang, F. H., and Zhang, Z. M., 2004, Petrography and metamorphic deformational history of the ultrahigh-pressure metamorphic rocks from the 100–2000 m core of Chinese Continental Scientific Drilling, China: Acta Petrologica Sinica, v. 20, p. 43–52.

You, Z. D., Su, S. G., Liang, F. H., Zhang, Z. M., 2005, The metamorphic evolution of the eclogitic rocks in the main hole of the Chinese Continental Scientific Drilling Project: An elucidation on the uplift processes of the ultrahigh-pressure metamorphic terrane: Acta Petrologica Sinica, v. 21, p. 381–388.

Zhang, R. Y., Hirajima, T., Banno, S., Cong, B. L., and Liou, J. G., 1995a, Petrology of ultrahigh-pressure rocks from the southern Su-Lu region, eastern China: Journal of Metamorphic Geology, v. 13, p. 659–675.

Zhang, R. Y., and Liou, J. G., 1997, Partial transformation of gabbro to coesite-bearing eclogites from Yangkou, the Sulu terrane, eastern China: Journal of Metamorphic Geology, v. 15, p. 183–202.

Zhang, R. Y., and Liou, J. G., 1998, Dual origin of garnet peridotites of Dabie-Sulu UHP terrane, eastern-central China: Episodes, v. 21, p. 229–234.

Zhang, R. Y., Liou, J. G., and Cong, B. L., 1994, Petrogenesis of garnet-bearing ultramafic rocks and associated eclogites in the Su-Lu ultrahigh-pressure metamorphic terrane, China: Journal of Metamorphic Geology, v. 12, p. 169–186.

Zhang, R. Y., Liou, J. G., and Ernst, W. G., 1995b, Ultrahigh-pressure metamorphism and decompressional P-T path of eclogites and country rocks from Weihai, eastern China: The Island Arc, v. 4, p. 293–309.

Zhang, R. Y., Liou, J. G., and Shu, J. F., 2002, Hydroxyl-rich topaz in high-pressure and ultrahigh-pressure kyanite quartzites, with retrograde woodhouseite, from the Sulu terrane, eastern China: American Mineralogist, v. 87, p. 445–453.

Zhang, R. Y., Liou, J. G., Tsujimori, T., and Maruyama, S., 2006, Non-UHP unit bordering the Sulu UHP terrane, eastern China: Transformation of Proterozoic granulite and gabbro to garnet amphibolite, *in* Hacker, B. R., McClelland, B., and Liou, J. G., eds., Ultrahigh-pressure metamorphism: Deep continental subduction: Geological Society of America Special Paper, v. 403, p. 169–206.

Zhang, R. Y., Liou, J. G., Yang, J. S., and Ye, K., 2003a, Ultrahigh-pressure metamorphism in the forbidden zone: The Xugou garnet peridotite, Sulu terrane, eastern China: Journal of Metamorphic Geology, v. 21, p. 539–550.

Zhang, R. Y., Liou, J. G., Zheng, Y. F., and Fu, B., 2003b, Transition of UHP eclogites to gneissic rocks of low-amphibolite facies during exhumation: Evidence from the Dabie terrane, central China: Lithos, v. 70, p. 1–23.

Zhang, R. Y., Yang, J. S., Wooden, J. L., Liou, J. G., and Li, T. F., 2005, U-Pb SHRIMP geochronology of zircon in garnet peridotite from the Sulu UHP terrane, China: Implications for mantle metasomatism and subduction-zone UHP metamorphism: Earth and Planetary Science Letters, v. 237, p. 729–743.

Zhao, R. X., Liou, J. G., Zhang, R. Y., and Wooden, J. L., 2005, SHRIMP U-Pb dating of zircon from the Xugou UHP eclogite, Sulu terrane, eastern China. International Geology Review, v. 47, p. 805–814.

Zhao, Z. Y., Wang, Q. C., and Cong, B. L., 1992, Coesite-bearing ultramafic pressure metamorphic rocks from Donghai, northern Jiangsu province, eastern China: "Foreign or i*n situ*?": Science in Geologica Sinica, v. 1, p. 43–58.

Zheng, Y. F., Fu, B., Gong, B., Li, L., 2003, Stable isotope geochemistry of ultrahigh pressure metamorphic rocks from the Dabie-Sulu orogen in China: Implications for geodynamics and fluid regime: Earth Science Reviews, v. 62, p. 105–161.